Humans Can Integrate Augmented Reality Feedback in Their Sensorimotor Control of a Robotic Hand

Francesco Clemente, Strahinja Dosen, Luca Lonini, Marko Markovic, Dario Farina, and Christian Cipriani

***Abstract*—Tactile feedback is pivotal for grasping and manipulation in humans. Providing functionally effective sensory feedback to prostheses users is an open challenge. Past paradigms were mostly based on vibro- or electrotactile stimulations. However, the tactile sensitivity on the targeted body parts (usually the forearm) is greatly less than that of the hand/fingertips, restricting the amount of information that can be provided through this channel. Visual feedback is the most investigated technique in motor learning studies, where it showed positive effects in learning both simple and complex tasks; however, it was not exploited in prosthetics due to technological limitations. Here, we investigated if visual information provided in the form of augmented reality (AR) feedback can be integrated by able-bodied participants in their sensorimotor control of a pick-and-lift task while controlling a robotic hand. For this purpose, we provided visual continuous feedback related to grip force and hand closure to the participants. Each variable was mapped to the length of one of the two ellipse axes visualized on the screen of wearable single-eye display AR glasses. We observed changes in behavior when subtle (i.e., not announced to the participants) manipulation of the AR feedback was introduced, which indicated that the participants integrated the artificial feedback within the sensorimotor control of the task. These results demonstrate that it is possible to deliver effective information through AR feedback in a compact and wearable fashion. This feedback modality may be exploited for delivering sensory feedback to amputees in a clinical scenario.**

***Index Terms*—Augmented reality (AR), motor learning, sensorimotor control, sensory substitution, visual system, wearable systems.**

I. Introduction

Mimicking the motor and sensory functions of a human hand using a prosthesis poses complex challenges in the fields of technology and applied neuroscience. While motor functions can be restored to a certain extent using a myoelectric prosthesis [1], providing functionally effective sensory feedback is a largely unsolved issue. In fact, none of the prostheses used in clinical practice, apart from a recently presented system (VINCENTevolution 2), have purposely designed closed-loop controllers with the user in the loop [2]. Control is achieved by the user by means of visual assessment and through feedback not intentionally implemented in the design (motor noise, socket pressure, harness, etc.). However, it is expected that prostheses would function better if their users could rely on an explicit artificial sensory feedback [3].

Sensory feedback can be provided invasively by interfacing directly with the neural structures normally involved in the control (e.g., the afferent nerve fibers) [4]–[7] or noninvasively by stimulating body sites normally not involved in the motor task [8]–[13]. While the first approach holds a potential of eliciting close-to-natural tactile sensations, noninvasive stimulation usually relies on the ability of the individual to learn to correctly interpret the stimuli. For example, the user needs to associate a specific intensity or frequency of stimulation delivered to the skin to the corresponding level of the prosthesis feedback variable, such as current grasping force (GF). In particular cases, this cognitive process can be less taxing, namely when the noninvasive stimulation targets reconstructed or remapped afferent physiological channels [14]–[16].

Among the noninvasive techniques, vibro- or electrotactile feedback have been widely investigated in the past as they do not require surgery, they elicit sensations that are well accepted by the users, and can be generated through miniaturized devices. In a typical configuration, small vibrators or electrodes are placed on the residual limb of the user (e.g., the forearm or the chest), and the sensory information from the sensors in the prosthesis is fed back to the individual by modulating one or multiple stimulation parameters (e.g., the intensity or the frequency of the vibration) based on the sensors readout, and on a specific encoding algorithm [2].

Regardless of how the information is processed, one of the main limitations of such techniques is that it is a challenging task for an individual to learn how to actually take advantage of it in daily activities. This applies to both noninvasive and invasive techniques; indeed, even after resuturing accidentally severed nerves and subsequent significant reinnervation of biological sensors occurs—that reasonably should be vastly superior to any artificial intra-neural sensory feedback—functional results are unsatisfactory unless the patient is in the early teens or younger [17]. In other words, even under “ideal” conditions, the limiting factor in sensory relearning is the patients’ ability to reinterpret the somatosensory information [18].

From an engineering perspective, there are two possible ways for addressing this limitation: exploiting a low-bandwidth feedback device [13], [19] or increasing the effective information throughput using multichannel configurations (which requires specific training of subjects to learn how to reinterpret the provided stimuli) [20]. In this work, we propose a new approach based on a simple and intuitive paradigm, which exploits the visual system. Providing visual feedback information is by far the most investigated technique in motor learning studies and generates learning effects superior to those observed with other stimulation modalities (i.e., haptic and auditory) [21].

Manuscript received March 7, 2016; revised June 24, 2016 and August 26, 2016; accepted September 17, 2016. Date of publication October 11, 2016; date of current version July 13, 2017. This work was supported by the European Commission under the NEBIAS (FP7-ICT-2013-10) and MYOSENS (FP7-PEOPLE-2011-IAPP-286208) projects. The work of L. Lonini was supported by the Max Näder Lab for Rehabilitation Technologies and Outcomes Research. This paper was recommended by Associate Editor J. del R. Millán.

F. Clemente and C. Cipriani are with the BioRobotics Institute, Scuola Superiore Sant’Anna, 56025 Pontedera, Italy (e-mail: f.clemente@sssup.it; ch.cipriani@sssup.it).

S. Dosen and M. Markovic are with the Biomedical Engineering Group, Clinic of Trauma Surgery, Orthopaedic Surgery and Plastic Surgery, University Medical Center Göttingen, Georg-August University, 37075 Göttingen, Germany (e-mail: strahinja.dosen@bccn.uni-goettingen.de; marko.markovic@bccn.uni-goettingen.de).

L. Lonini is with the Max Näder Lab for Rehabilitation Technologies and Outcomes Research, Rehabilitation Institute of Chicago, Chicago, IL 60611 USA (e-mail: llonini@ricres.org).

D. Farina is with the Department of Bioengineering, Imperial College London, London, SW7 2AZ, U.K. (e-mail: d.farina@imperial.ac.uk).

Color versions of one or more of the figures in this paper are available online at http://ieeexplore.ieee.org

Digital Object Identifier 10.1109/THMS.2016.2611998

However, due to technological limitations, the translation of artificial visual feedback to the prosthetic field was so far rather poor as, until the recent advent of augmented reality (AR) goggles (e.g., Google Glass and Microsoft HoloLens), it was impractical to provide enhanced visual feedback to an individual in a compact and wearable fashion. Now, the scenario is different and AR technology is evolving at a fast pace, inviting studies in which augmented vision is used and assessed in different applications, including closed-loop prostheses. In line with this approach, Engeberg and Meek proposed to convey grip force (GF) information of a myoelectric prosthesis through a visual interface, modulating the intensity of the light of a light-emitting diode (LED) mounted on the thumb [22]. They evaluated the system with six able-bodied participants and showed that the visual feedback of force improved the performance when manipulating a brittle test object. Interestingly, the novel LED-based feedback showed to be beneficial, albeit the participants received it in addition to watching and hearing the prosthesis. However, one can argue that their approach enforces the user to closely pay visual attention to the prosthesis, since he/she needs to register the modulation of the intensity of a miniature light source; this worsens the problem that artificial feedback tries to solve, i.e., reduce the visual attention on the prosthesis needed to control it. Additionally, the needed level of attention could be even higher than in the absence of feedback, making the method cognitively taxing. Markovic *et al.* presented a system for the semiautonomous control of hand prostheses, which displayed feedback about hand aperture using AR glasses, granting thereby the possibility to receive the feedback even without watching the prosthesis [23]. Their tests showed that able-bodied participants were able to properly interpret the AR feedback and to correct artificially induced errors in the hand aperture of the prosthesis, without looking at the hand but gave no clue about the ability of the participants in incorporating the visual information in their own sensorimotor control.

Building on this previous work, we have investigated whether artificial sensory feedback represented using AR is integrated into the sensorimotor control of a grasping task. To this end, we designed a paradigm, in which healthy humans operated a robot hand to lift and reposition an object. In addition, our system displayed via see-through AR glasses continuous artificial visual feedback in the form of an ellipse, by scaling its horizontal and vertical axes according to the measured grip closure (GC) and GF, respectively. Notably, the task was performed under visual control, and it was known by previous studies that it could be readily completed even without the augmented feedback [19]; hence, the AR feedback was not only artificial but also redundant. Nevertheless, because of the intuitiveness of the visual feedback provided, we expected that the participants would readily integrate it into their sensorimotor control of the robotic hand. To reveal such integration, we implemented a well-established protocol used in our previous studies [13], [19] as well as in the literature on adaptation in motor control [24]. We modified, unknowingly to the participants, the way we translated the GF or the GC into visual cues in blocks of catch trials after first training the participants.

Our results showed that participants mastered the task and integrated the AR feedback within 200 repetitions. When the visual feedback of the GF was modified, they adapted their behavior accordingly, whereas the modification of the visual feedback of the GC did not produce visible differences, suggesting that the proportions of the ellipse did not influence the perception of the axis representing the GF. Adding the AR feedback also resulted in more consistent performance across grasping trials. Therefore, these outcomes are optimistic with respect to the application of AR interfaces in closed-loop prosthetics, inviting further studies in which more advanced AR feedback paradigms are assessed and exploited.

II. Materials

Eight able-bodied participants were enrolled in the study (all males, aged between 27 and 35, one left handed). Informed consent according to the declaration of Helsinki was obtained before conducting the study. The experimental setup consisted of a robot hand, a data glove, an instrumented test-object and a stand, a pair of AR glasses, and a PC running a custom application [see Fig. 1(a)]. The robot hand was a right-handed version of the IH2 Azzurra hand (Prensilia SRL, Italy), in which the only allowed movements were the flexion/extension of the thumb and index finger, in order to allow stable pinch grasps between the thumb and the index. The participants wore a splint that allowed them to maneuver the robotic hand with their own arm. They also controlled in a master–slave fashion the position of the robotic digits through the data glove (Cyberglove, Cyberglove Systems, San Jose, CA, USA) by moving their own thumb and index finger in a thumb–index virtual pinch grip. The AR glasses were the M100 Smart Glasses (Vuzix Corp., Rochester, NY, USA) integrating single-eye display used to project the AR feedback to the participant during the manipulation task (as described below). The position of the display (400×240 pixel resolution and equivalent to a 4-in mobile device screen seen at 14-in distance) was adjusted manually for each participant so that the AR feedback was located in the peripheral vision, thereby avoiding the interference with the central scene including the hand and target object [see Fig. 1(b)]. Notably, the images visualized on the screen appear to be transparent.

The same test object as in [19] and [25] was used in this experiment. It consisted of a rigid plastic block ($55 \times 40 \times 50$ mm; 105 g) covered by plastic plates, equipped with piezoresistive force sensors (FsG series, Honeywell, MN; 0–15 N; 0–2 kHz) able to measure the GF exerted on each plate by the thumb and index robotic digits independently. The stand was instrumented with a similar sensor, which allowed calculating the load force (LF) exerted by the user on the object as long as it was in contact with the stand itself (i.e., until lift-off).

The PC acquired the sensors signals (GF and LF) through a data acquisition board (USB-6002, National Instruments Corp., Austin, TX, USA) and handled a bidirectional serial communication (RS-232) with the robotic hand and with the data glove. Finally, the AR glasses were connected to the PC through a USB connection and their display was used as an external monitor. On the PC, a custom C application (LabWindows/CVI, National Instruments Corp.) translated sensory information into appropriate control commands for the robotic hand and into visual information for the AR glasses to display. The whole control loop was updated at a rate of 90 Hz, which was the maximum allowed by the system.

III. Methods

The participants, standing in front of a bench, were instructed to repeatedly grip, lift, replace, and release the test object at a self-selected speed. Specifically, their task consisted of:

1) moving their right arm to reach the object with the robot hand mounted on the splint (see Fig. 1);
2) moving their own thumb and index finger to control the robot hand so that it eventually grasped the object;
3) lifting the test object a few centimeters above the stand;
4) putting the test object back on the stand;
5) releasing the object by opening their grasp.

During the experiment, which was divided in series of trials, the participants received grasp-related information (GF and GC) through the AR glasses [green ellipse; see Fig. 1(a)].

The control was implemented in a way that the grip aperture of the robotic hand duplicated the grip aperture of the individual's own

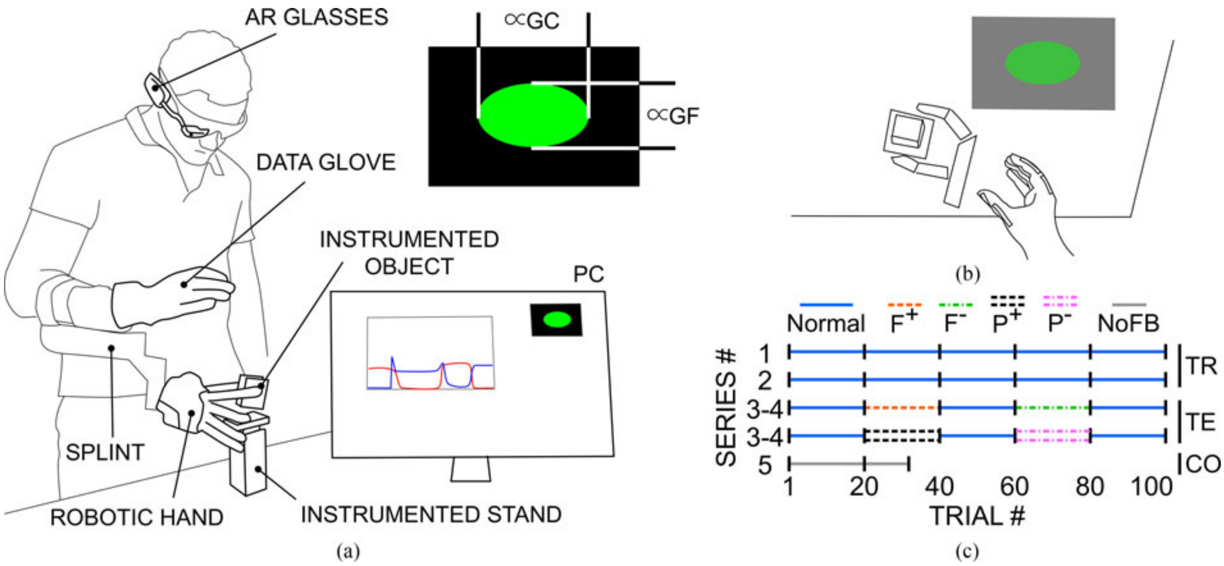

Fig. 1. Experimental setup. (a) Participant performing the pick-and-lift task of an instrumented object by controlling the robotic hand through the data glove. Among other information, the GF exerted on the instrumented object and the robotic GC were recorded by a PC and used to compute and deliver sensory feedback information (inset) to the participant through AR glasses. The screen of the PC monitor was visible only to the experimenter. (b) Scene as seen by the participant. The adjustable screen of the AR glasses allowed placing the AR feedback in the peripheral sight without interfering with the instrumented object and robotic hand view. (c) Each participant performed four series of 100 trials (divided in blocks of normal and different types of catch trials, where the AR feedback was manipulated) plus a fifth series of 30 trials performed without AR feedback (NoFB, gray). F^+, F^-, P^+, and P^- denote the type of the catch trial (see text). The order of the third and fourth series was randomized among participants. TR, TE, and CO denote the name of the experiment phase, i.e., training, test, and control, respectively.

hand. To achieve this, the positions of the robotic digits were controlled using the flexion/extension information recorded from the individuals' metacarpophalangeal (MCP) and proximal interphalangeal (PIP) joints by the data glove. In particular, the target position TP_d of the robotic digit *d* was computed as

$$TP_d = (MCP_d + PIP_d)\ k_d + C_d, \qquad \text{with } d = 1, 2 \tag{1}$$

where MCP_d and PIP_d are the measured human joint angles, k_d is a transformation gain, and C_d is an offset. The parameter k_d was calibrated for each participant individually at the beginning of the experiment in order to map his/her own hand aperture to the robotic hand range of motion, so as to ensure intuitive controllability over the robotic digits. The offset C_d was randomly generated trial-by-trial by the computer application to produce a random initial flexion of the robotic digit with respect to the human fingers. In particular, C_d was computed in order to generate an angular offset uniformly distributed within the interval $[-10°, 10°]$. Accordingly, in each trial, the mapping between the human and the robotic hand grip aperture differed; the exact initial position of the robotic fingers was, therefore, unpredictable to the user. As in [19], this unpredictable mapping was included in order to simulate an amputee (who lacks in proprioception) operating a myoelectric prosthesis. In fact, the random mapping impeded the participants to operate the hand by using learned digit positions.

Once the robot digits touched the test object, they could no longer move due to the interaction with the object, and forces normal to its sides (GF) were generated to levels that depended on the participant grip aperture (0.2 $N/°$).

The participants received a real-time compound visual feedback from the robotic hand onto the screen of the AR glasses in the form of a green-colored ellipse. The size of the ellipse (its axes lengths) varied based on the measured GC and GF of the robotic hand, updated at a rate of 90 Hz (see Fig. 1). In particular, the width W_e of the ellipse (in pixels) represented the GC and was computed as

$$W_e = (CP_{\mathrm{RT}} + CP_{\mathrm{RI}})\ k_W + R_W \tag{2}$$

where $\mathrm{CP}_{\mathrm{RT}}$ and $\mathrm{CP}_{\mathrm{RI}}$ were the actual positions of the robotic thumb and index, k_W is a transformation constant, and R_W is the ellipse width at rest (i.e., when both digits are fully extended and, in turn, $\mathrm{CP}_{\mathrm{RT}} = \mathrm{CP}_{\mathrm{RI}} = 0$). The height of the ellipse H_e was modulated by the GF

$$H_e = (GF_{\mathrm{RT}} + GF_{\mathrm{RI}})\ k_H + R_H \tag{3}$$

where $\mathrm{GF}_{\mathrm{RT}}$ and $\mathrm{GF}_{\mathrm{RI}}$ denote the forces generated by the robotic thumb and index, respectively, as measured by the instrumented object, k_H is a transformation constant, and R_H is the ellipse height when there is no contact with the object (i.e., $\mathrm{GF}_{\mathrm{RT}} = \mathrm{GF}_{\mathrm{RI}} = 0$). In practice, during the execution of the task, the ellipse would 1) increase its W_e, while the robotic digits closed toward the test object (with $H_e = R_H$) and, once the digits were in contact with it, 2) increase its H_e as they applied enough GF to lift the object (with W_e constant and related to the width of the object). During replace and release, the evolution of the ellipse shape was opposite (see Fig. 2).

A trial was considered successful if the participant was able to perform the task while avoiding that the GF (i.e., $\mathrm{GF}_{\mathrm{RT}} + \mathrm{GF}_{\mathrm{RI}}$) exceeded a fixed breaking threshold (experimentally set to 2.4 N). If the participant generated a suprathreshold GF, the instrumented object virtually broke; this was clearly signaled to the participant by the robotic hand (as it automatically reopened) and by the ellipse, which was replaced by a red-colored static circle, displayed on the AR glasses until the user started a new trial (by reopening their own hand). The breaking threshold was introduced in order to prevent the participants adopting a strategy, in which they grasped the object by simply closing the robot digits as much as possible, as in [19].

The protocol included two series of 100 trials (training phase), two additional series of 100 trials (test phase), and a final series of 30

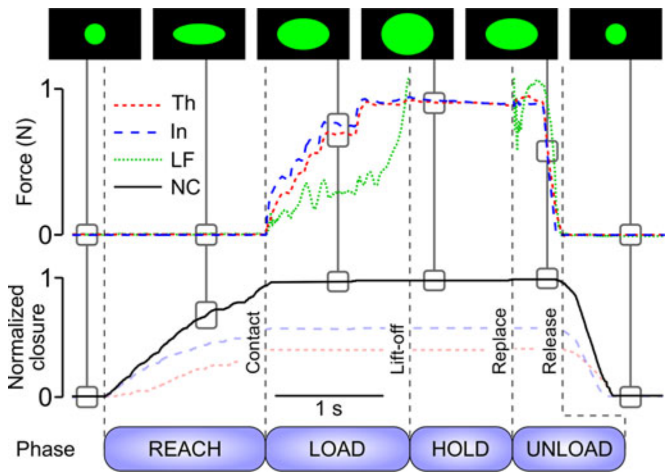

Fig. 2. Single pick-and-lift trial. In descending order, the temporal evolution of AR feedback, GF/LF, and robotic fingers/hand closure (normalized to object width). Bottom: manipulation task phases. Gray boxes show the connection between the relevant variables and the shape of the resulting AR feedback. Th/In indicates the (GF and closure) traces related to the thumb/index, LF the load force, and NC the normalized closure of the robotic hand. Vertical dashed lines indicate the mechanical events delimiting task phases.

trials (control phase) with 5–10-min breaks between the series [see Fig. 1(c)]. If the failure rate of the first series of the training phase was below 30%, the participant was deemed sufficiently skilled and he/she proceeded to the test phase directly (thus skipping one training series). During the training phase, the modulation of the visual feedback was consistent across all trials (we dubbed these normal trials). During the test phase, normal trials were interleaved with blocks of catch trials [see Fig. 1(c)], in which the modulation of the visual feedback was manipulated. Specifically, the parameter *k* in (2) or (3) was modified, unknowingly to the participants, to obtain different effects as explained below. In the control phase, the visual feedback was turned OFF (i.e., NoFB trials; see Fig. 1(c)], in order to compare the outcomes with and without visual feedback. The catch trials in the test phase were conceived to verify whether the participants incorporated the new sensory feedback and if they adapted their motor plan accordingly. Four types (and blocks) of catch trials were introduced.

1) F^+ *catch trials*: The GF displayed to the participant, namely the height of the ellipse H_e, was 30% lower than in normal trials (i.e., $k_H|_{\mathrm{F+}} = 0.7\,k_H|_{\mathrm{normal}}$). In response to this perturbed feedback, we expected that the participants would apply a larger GF, in order to match the height H_e learned previously (during the training phase). Hence, in this particular case, we increased the breaking threshold of the test object by the same percentage.
2) F^- *catch trials*: The GF displayed to the participant (again, H_e) was 30% higher than in normal trials (i.e., $k_H|_{\mathrm{F-}} = 1.3\,k_H|_{\mathrm{normal}}$). We hypothesized that the participants would reduce their GF in order to match the previously learned H_e.
3) P^+ *catch trials*: The GC displayed to the participant (the width of the ellipse W_e) was 30% lower than in normal trials (i.e., $k_W|_{\mathrm{P+}} = 0.7\,k_W|_{\mathrm{normal}}$). This condition tested whether the interpretation of GF (the height of the ellipse) was affected by a change in the proportions of the ellipse. As the GC was not a task-relevant variable, we did not expect behavioral changes unless participants relied on the compound information contained in the ellipse (i.e., the overall shape), rather than on the single variables (axes lengths).
4) P^- *catch trials*: The GC displayed to the participant (with W_e) was 30% higher than in normal trials (i.e., $k_W|_{\mathrm{P-}} = 1.3\,k_W|_{\mathrm{normal}}$). The assumptions were the same as for the previous condition.

Catch trials were organized in blocks of 20 consecutive trials, each block being separated from the other by at least a block of 20 normal trials. In particular, one series of the test phase contained F^+ and F^- catch trials, whereas the other included P^+ and P^- catch trials. The order of the two series was randomized among participants [see Fig. 1(c)]. Participants were unaware of the catch trials.

IV. Data Analysis

All data were digitized and stored for offline analysis. Each trial was defined as successful or not. Unsuccessful trials were those in which the participant failed to lift the object or applied excessive GFs. For each participant, we analyzed the data from the test and control phases. The time between the moments of the first digit contact (i.e., when GF > 0) and lift-off (i.e., when the contact between the test object and the stand was broken) was determined and defined as the load phase duration (see Fig. 2). The GF at lift-off and the load phase duration, which are known to be relevant variables in the pick-and-lift task [26], were used to compare the participants' behavior between conditions (normal, catch, and NoFB trials).

The Kolmogorov–Smirnov (KS) test was used to verify that the data were normally distributed. If so, intraparticipant comparisons between normal and NoFB trials were performed using an unpaired two-sample *t*-test, while a paired two-sample *t*-test was used for interparticipant analyses. If the KS test indicated a different distribution of the data, a Wilcoxon rank-sum/signed rank test was used in place of the unpaired/paired two-sample *t*-test. In order to reduce biases introduced by fatigue and effects of catch trials, the first 20 NoFB trials were compared to the first 20 normal trials from the last series of the test phase.

Additionally, a repeated-measures analysis of variance (ANOVA) was performed in order to highlight differences among the six experimental conditions (normal, F^+, F^-, P^+, P^-, and NoFB) in case the KS test indicated that the data were normally distributed. If the ANOVA suggested that there was a significant difference among groups, those were compared pairwise after a Tukey–Kramer correction for multiple comparisons.

In all cases, a p value <0.05 was considered for statistical significance. When nonparametric tests were used, the power of the test was calculated following the approximation proposed by Lehmann and Abrera [27].

V. Results

The KS test demonstrated that the distribution of all data, apart from the load phase duration, did not deviate significantly from the normal distribution.

The participants readily mastered the task within 200 repetitions; four of them demonstrated learned behavior already in the first series, hence skipped the second training series. At the end of the training phase (last 50 trials), the average failure rate for the participants was less than 20%.

We looked at the temporal evolution of the GF in each condition (see Fig. 3), synching the data on two mechanical events: the time when the last digit made contact with the object and lift-off. Compared to normal trials, the GF was higher during F^+ catch trials and lower during F^- catch trials (see the first row in Fig. 3), while there were no significant changes in the GF during P^+ and P^- catch trials (see the second row in Fig. 3). For this particular participant, when the AR feedback was not

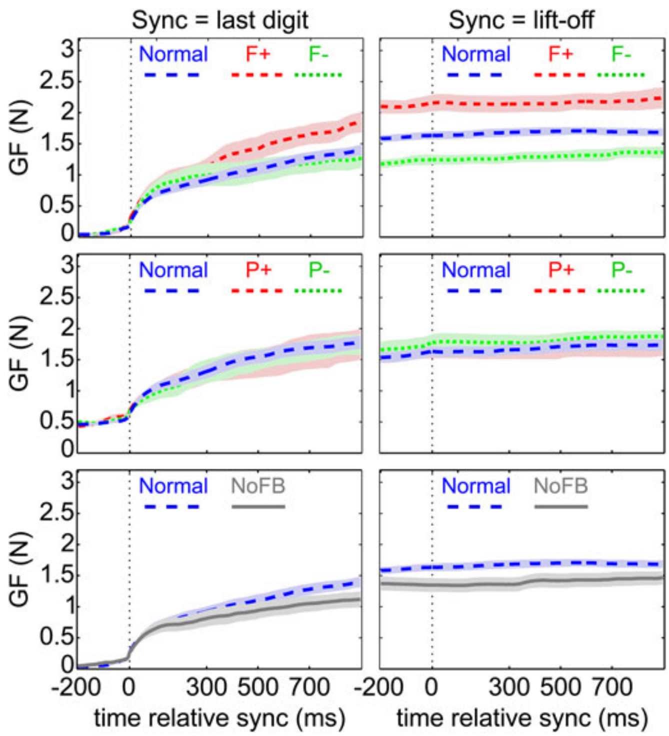

Fig. 3. Effect of catch and NoFB trials on the temporal evolution of the GF for a representative participant. The GF was affected when, unknowingly to the participant, the mapping between the GF and the AR feedback was modified (F^+ and F^- catch trials, first row). The same effect was not observed when the feedback related to GC was modified (P^+ and P^- catch trials, second row). When the AR feedback was turned OFF (NoFB condition, last row), the participant applied a lower GF at lift-off with increased variability (when compared to normal trials from the previous session). Vertical dotted lines represent the sync event (left: last digit to make contact; right: lift-off). Solid lines represent the mean and shaded areas are 95% confidence intervals.

provided (NoFB trials), the GF at lift-off was lower when compared to normal trials from the previous series (see the third row in Fig. 3).

Similar trends were observed across all participants [see Fig. 4(a)]: the repeated-measures ANOVA reported a significant effect of the test condition ($F(5, 35) = 15.7$, $p < 0.001$). The posthoc analysis revealed a statistical difference between normal and F^+ and F^- catch trials, with the participants generating higher GF in F^+ catch trials ($p < 0.001, \beta < 0.001$) and lower GF in F^- catch trials ($p < 0.05$, $\beta = 0.0037$) when compared to normal trials. No significant changes were observed for P^+ and P^- catch conditions ($p > 0.05, \beta = 0.04$, and 0.08 respectively). No differences between normal and NoFB trials were found at group level as well ($p > 0.05$, $\beta = 0.1$).

Notably, participants adapted their behavior to the changes in the AR feedback (when switching from one condition to another) immediately on the first trial of the block, as the GF median value immediately changed in presence of the new condition [see Fig. 4(b)].

Furthermore, participants took advantage of the AR feedback to obtain stable performance when repeating the pick-and-lift task. Indeed, by comparing the IQR of the GF at lift-off between normal and NoFB trials (paired two-sample *t*-test), we found that this was significantly higher than when the AR feedback was present (normal trials) [$t(7) = 2.6$, $p < 0.05$, $\beta = 0.0045$; see Fig. 5(a)], confirming that the AR feedback improved the consistency of participants in performing the motor task.

Finally, we compared the load phase duration between normal and NoFB trials for all participants and found it to be shorter in NoFB trials (Wilcoxon signed rank test, $Z(36) = 2.52$, $p < 0.01$, and $\text{power} = 0.91$). Therefore, the AR feedback seemed to reduce the participants' speed at performing the manipulation task significantly [see Fig. 5(b)].

VI. Discussion

We trained participants to pick, lift, and replace an instrumented object by operating a robotic hand through a data glove. In addition to seeing the hand and the object, participants wore AR glasses that provided enhanced visual feedback on the grasp parameters, i.e., GF and GC. The AR feedback was shown as an ellipse, with the axes proportional to the two variables, displayed in peripheral vision during the task. We hypothesized that participants will integrate the AR feedback in their sensorimotor control of the task, following a short training comprised of repeated grasping trials. In order to test this hypothesis, we introduced disturbances in the feedback by upscaling or downscaling the ellipse axis corresponding to GF and found that participants scaled the actual GF accordingly (see Figs. 3 and 4), proving that the AR feedback was used to execute the motor task. On the contrary, rescaling the feedback of GC did not alter their motor commands. This suggests that participants decoupled the two variables even if they were delivered together in the form of an ellipse: a change in the proportions of the ellipse did not affect the participants' behavior.

Although the AR feedback was redundant and not strictly required to complete the task, it was readily incorporated in the sensorimotor control of the task. We argue that the AR feedback was intuitive, and thus, participants readily learned the processes of sensory substitution needed to take advantage out of it. This is supported by the particularly short training phase required in order to master the task: four of the participants needed a single series of 100 trials (which lasted around 10 min). This is remarkably low if compared to our previous study [19], in which participants were provided with vibrotactile feedback while executing the same pick-and-lift task; in that case, five series of 100 trials were needed to integrate the artificial feedback.

The significant difference in the variability of the GF at lift-off, between the normal and NoFB conditions, further demonstrates the incorporation of the AR feedback. In the NoFB condition, participants had no information on the GF produced on the (stiff) test object and could complete the task only through incidental stimulation. In turn, the variability of GF increased, indicating thereby a less consistent motor performance. Instead, when the AR feedback was activated, the participants had specific information on task-relevant variables, which allowed them to execute the task in a more consistent manner. This is in line with the suggestion by Nowak *et al.* [28] that the efficiency of feedback for predictive movement planning is specific to the effector and the regulated variable, i.e. (non-AR) visual feedback may be useful to adjust arm movement kinematics, but less helpful for the regulation of GF.

The enhanced visual feedback did affect the time needed to lift the object (i.e., the load phase duration) compared to NoFB trials. This is in line with previous research, in which the task speed was reduced when the feedback was turned ON [29], [30]. Additionally, the typical (median) load phase duration found in this setup [see Fig. 5(b)] was tripled when compared to mature grasping by healthy humans (1.2 versus 0.4 s) [31] and doubled if compared to our previous experiments (0.6 s) [19]. In addition, behavioral changes in the way the participants grasped the test object could be observed already at the first catch trial (see Fig. 4). These findings suggest that the participants did not execute feed-forward stereotypical movements based on a previously learned model of the task, using instead a "safer" and slower feedback strategy. As demonstrated in motor control studies of grasping in

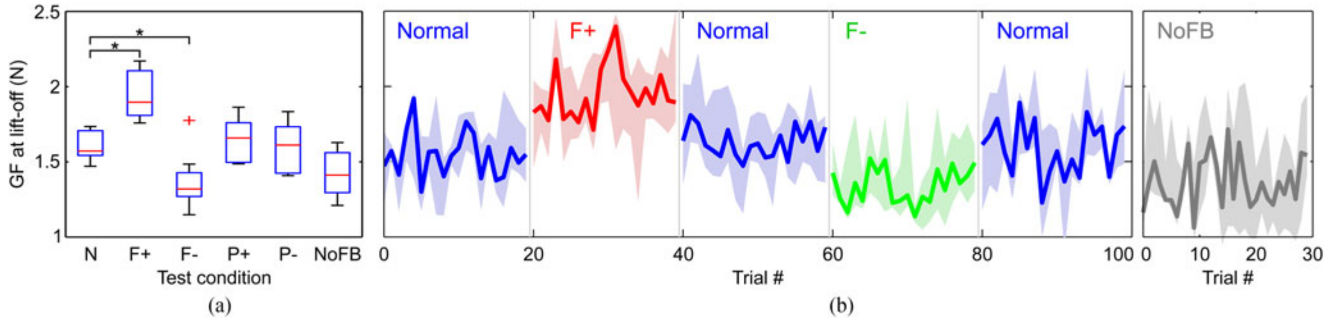

Fig. 4. Effect of catch and NoFB trials on the GF at lift-off across all participants. (a) Distribution of the GF at lift-off across all participants in each condition. (b) Median GF at lift-off across all participants as a function of trial number (shaded areas represent IQR). Of notice, the GF was affected already on the first catch trial in each block. * indicates $p < 0.05$.

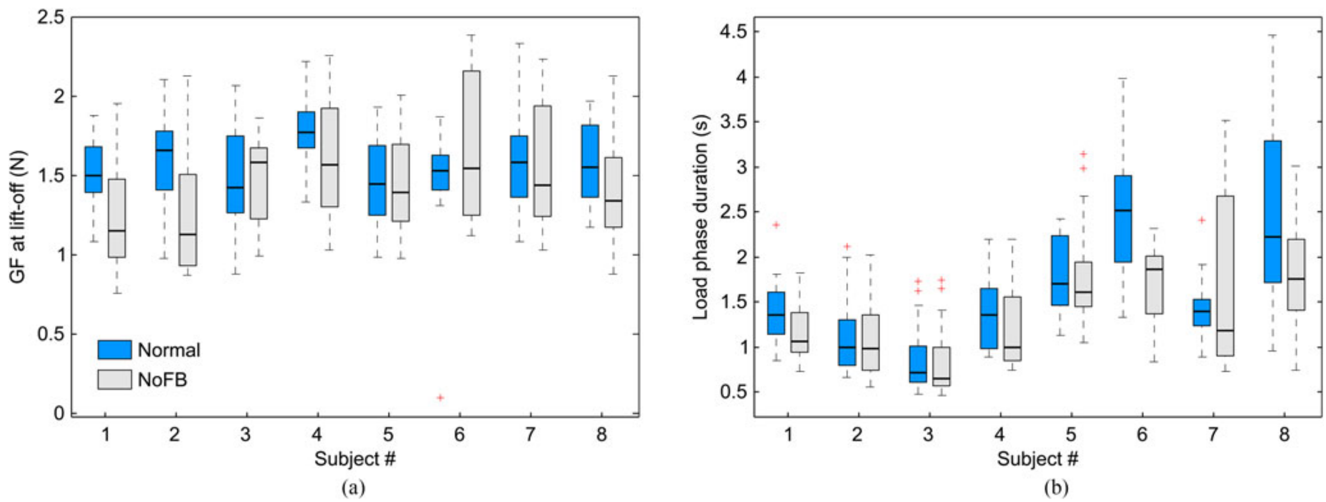

Fig. 5. Comparison of GF at lift-off and load phase duration between normal (blue) and NoFB (gray) trials for each participant. (a) When the AR feedback is not available, the GF variability (IQR) increases and therefore repeatability performance of the participants on the task is degraded. (b) Load phase duration decreases significantly when the AR feedback is removed, suggesting that the AR feedback is cognitively taxing.

able-bodied humans, if a feed-forward model would have been used, as catch trials introduced a misleading cue (there was a discrepancy between the desired and actual GF), the participants could not adapt to the new perturbed condition in a single trial [32], [33]. Moreover, it is known that continuous closed-loop control of dynamic motor behaviors is possible only at frequencies below 1 Hz, due to neural delays [34], and this could explain the substantial increase in the load phase duration observed in the present study. This outcome might be due to the relatively limited duration of the experiment and the fact that the sensory feedback was provided in a continuous fashion. This hypothesis is supported by our previous study [19], where the longer training and the time-discrete feedback (as opposed to continuous feedback) allowed the participants to build a feed-forward model, which resulted in a shorter load phase duration (almost matching the performance observed in healthy humans). Additionally, such result is in line with previous studies in motor learning: for simple tasks, continuous visual feedback provided during the task is known to lead to a dependence on the feedback, which might be detrimental to the development of an internal motor representation of the task [21].

Although GC was a redundant control variable in this experiment, proprioception can be helpful to reduce visual attention needed by participants in activities of daily living involving grasping and manipulation. Whether this paradigm can provide such an advantage should be investigated in future studies. For example, handling objects with different compliances could be used to probe if the AR feedback allows learning an internal model of the GF [35].

The fact that participants reacted differently to the individual perturbations of the GC and GF feedback has a practical relevance, since this implies that AR feedback can be provided in a compact form. Such feedback could include multiple variables to provide comprehensive information about the state of the prosthesis and/or highly dynamic signals such as feedback on EMG to allow for predictive control, as demonstrated in a recent study [36]. This is an advantage over other feedback paradigms particularly in the case of multiarticulated prostheses with independently controllable degrees of freedom [37] that could require more sophisticated feedback systems. Additionally, when considering a greater number of variables or higher bandwidth of the transmitted signals, the advantage of AR feedback over traditional solutions is twofold: first, it is not influenced by the same drawbacks of other feedback paradigms, such as increased power consumption, bulkiness, and weight (e.g., an array of vibrators would be needed in order to code the additional information, while with AR feedback the visual output can just be recoded); secondly, because of the larger bandwidth of the communication channel, the effectiveness of visual feedback increases with task complexity [21]. We, thus, invite further studies which exploit the advantages of such paradigm in a more complex task framework.

In the previous study [23], the AR feedback was used in combination with a semiautonomous control system integrating a simple proportional myoelectric control. However, the setup was rather bulky, with the participants looking at nontransparent stereoscopic displays and thereby observing the scene as a 3-D video stream. Furthermore, the projected feedback transmitted only the grip aperture. The sensory feedback system presented in this study is closer to an end-user application, since the feedback was provided nonintrusively via peripheral vision, and using a simple visual form, which turned out to be easy to perceive and understand. A similar setup could be readily translated into a clinical scenario: the AR feedback could be easily generated by an app installed in the AR glasses and a Bluetooth communication between the AR glasses and the prosthesis would transmit the relevant information to the feedback app. Given the recent developments in wearable computing, it is highly likely that such devices will become common in the near future.

Acknowledgment

The authors would like to thank Dr. F. Cavallo for providing the augmented reality glasses used in this work.

References

[1] R. F. ff. Weir and J. W. Sensinger, "Design of artificial arms and hands for prosthetic applications," in *Standard Handbook of Biomedical Engineering and Design*. New York, NY, USA: McGraw-Hill, 2003, pp. 537–598.

[2] C. Antfolk, M. D'Alonzo, B. Rosén, G. Lundborg, F. Sebelius, and C. Cipriani, "Sensory feedback in upper limb prosthetics," *Expert Rev. Med. Devices*, vol. 10, no. 1, pp. 45–54, 2013.

[3] D. S. Childress, "Closed-loop control in prosthetic systems: Historical perspective," *Ann. Biomed. Eng.*, vol. 8, nos. 4–6, pp. 293–303, 1980.

[4] G. S. Dhillon and K. W. Horch, "Direct neural sensory feedback and control of a prosthetic arm," *IEEE Trans. Neural Syst. Rehabil. Eng.*, vol. 13, no. 4, pp. 468–472, Dec. 2005.

[5] M. J. Ortiz-Catalan, B. Håkansson, and R. Brånemark, "An osseointegrated human-machine gateway for long-term sensory feedback and motor control of artificial limbs," *Sci. Transl. Med.*, vol. 6, no. 257, p. 257re6, 2014.

[6] S. Raspopovic *et al.*, "Restoring natural sensory feedback in real-time bidirectional hand prostheses," *Sci. Transl. Med.*, vol. 6, no. 222, p. 222ra19, 2014.

[7] D. W. Tan, M. A. Schiefer, M. W. Keith, J. R. Anderson, J. Tyler, and D. J. Tyler, "A neural interface provides long-term stable natural touch perception," *Sci. Transl. Med.*, vol. 6, no. 257, p. 257ra138, Oct. 2014.

[8] R. W. Mann and S. D. Reimers, "Kinesthetic sensing for the EMG controlled 'Boston Arm,'" *IEEE Trans. Man-Mach. Syst.*, vol. 11, no. 1, pp. 110–115, Mar. 1970.

[9] A. Chatterjee, P. Chaubey, J. Martin, and N. Thakor, "Testing a prosthetic haptic feedback simulator with an interactive force matching task," *J. Prosthetics Orthotics*, vol. 20, no. 2, pp. 27–34, 2008.

[10] I. Saunders and S. Vijayakumar, "The role of feed-forward and feedback processes for closed-loop prosthesis control," *J. Neuroeng. Rehabil.*, vol. 8, no. 1, p. 60, 2011.

[11] S. Dosen, A. Ninu, T. Yakimovich, H. Dietl, and D. Farina, "A novel method to generate amplitude-frequency modulated vibrotactile stimulation," *IEEE Trans. Haptics*, vol. 9, no. 1, pp. 3–12, Jan.–Mar. 2015.

[12] C. Antfolk, A. Björkman, S. O. Frank, F. Sebelius, G. Lundborg, and B. Rosen, "Sensory feedback from a prosthetic hand based on air-mediated pressure from the hand to the forearm skin," *J. Rehabil. Med.*, vol. 44, no. 8, pp. 702–707, 2012.

[13] F. Clemente, M. D'Alonzo, M. Controzzi, B. B. Edin, and C. Cipriani, "Non-invasive, temporally discrete feedback of object contact and release improves grasp control of closed-loop myoelectric transradial prostheses," *IEEE Trans. Neural Syst. Rehabil. Eng.*, to be published, doi: 10.1109/TNSRE.2015.2500586.

[14] T. A. Kuiken, P. D. Marasco, B. A. Lock, R. N. Harden, and J. P. A. Dewald, "Redirection of cutaneous sensation from the hand to the chest skin of human amputees with targeted reinnervation," *Proc. Nat. Acad. Sci. USA*, vol. 104, no. 50, pp. 20061–20066, 2007.

[15] C. Antfolk *et al.*, "Artificial redirection of sensation from prosthetic fingers to the phantom hand map on transradial amputees: Vibrotactile versus mechanotactile sensory feedback," *IEEE Trans. Neural Syst. Rehabil. Eng.*, vol. 21, no. 1, pp. 112–120, Jan. 2013.

[16] J. S. Schofield, K. R. Evans, J. P. Carey, and J. S. Hebert, "Applications of sensory feedback in motorized upper extremity prosthesis: A review," *Expert Rev. Med. Devices*, vol. 11, no. 5, pp. 1–13, 2014.

[17] G. Lundborg, "Nerve injury and repair - A challenge to the plastic brain," *J. Peripher. Nerv. Syst.*, vol. 8, no. 4, pp. 209–226, 2003.

[18] B. Rosen, G. Lundborg, L. B. Dahlin, J. Holmberg, and B. Karlson, "Nerve repair: Correlation of restitution of functional sensibility with specific cognitive capacities," *J. Hand Surgery Brit. Eur. Vol.*, vol. 19, no. 4, pp. 452–458, 1994.

[19] C. Cipriani, J. L. Segil, F. Clemente, R. F. Weir, and B. B. Edin, "Humans can integrate feedback of discrete events in their sensorimotor control of a robotic hand," *Exp. Brain Res.*, vol. 232, no. 11, pp. 3421–3429, 2014.

[20] M. D'Alonzo, S. Dosen, C. Cipriani, and D. Farina, "HyVE—hybrid vibro-electrotactile stimulation—is an efficient approach to multi-channel sensory feedback," *IEEE Trans. Haptics*, vol. 7, no. 2, pp. 181–90, Apr.–Jun. 2014.

[21] R. Sigrist, G. Rauter, R. Riener, and P. Wolf, "Augmented visual, auditory, haptic, and multimodal feedback in motor learning: A review," *Psychon. Bull. Rev.*, vol. 20, no. 1, pp. 21–53, 2013.

[22] E. D. Engeberg and S. Meek, "Enhanced visual feedback for slip prevention with a prosthetic hand," *Prosthetics Orthotics Int.*, vol. 36, no. 4, pp. 423–429, 2012.

[23] M. Markovic, S. Dosen, C. Cipriani, D. Popovic, and D. Farina, "Stereovision and augmented reality for closed-loop control of grasping in hand prostheses," *J. Neural Eng.*, vol. 11, no. 4, 2014, Art. no. 046001.

[24] R. Shadmehr, M. A Smith, and J. W. Krakauer, "Error correction, sensory prediction, and adaptation in motor control," *Annu. Rev. Neurosci.*, vol. 33, pp. 89–108, 2010.

[25] A. Panarese, B. B. Edin, F. Vecchi, M. C. Carrozza, and R. S. Johansson, "Humans can integrate force feedback to toes in their sensorimotor control of a robotic hand," *IEEE Trans. Neural Syst. Rehabil. Eng.*, vol. 17, no. 6, pp. 560–567, Dec. 2009.

[26] R. S. Johansson and B. B. Edin, "Predictive feed-forward sensory control during grasping and manipulation in man," *Biomed. Res.*, vol. 14, pp. 95–95, 1993.

[27] E. L. Lehmann and H. J. D'Abrera, *Nonparametrics: Statistical Methods Based on Ranks*. San Francisco, CA, USA: Holden-Day, 1975.

[28] D. Nowak, S. Glasauer, and J. Hermsdörfer, "How predictive is grip force control in the complete absence of somatosensory feedback?" *Brain*, vol. 127, no. 1, pp. 182–192, 2004.

[29] C. E. Stepp and Y. Matsuoka, "Relative to direct haptic feedback, remote vibrotactile feedback improves but slows object manipulation," in *Proc. Annu. Int. Conf. IEEE Eng. Med. Biology Soc.*, 2010, pp. 2089–2092.

[30] H. J. B. Witteveen, F. Luft, J. S. Rietman, and P. H. Veltink, "Stiffness feedback for myoelectric forearm prostheses using vibrotactile stimulation," *IEEE Trans. Neural Syst. Rehabil. Eng.*, vol. 22, no. 1, pp. 53–61, Jan. 2014.

[31] R. S. Johansson and J. R. Flanagan, "Coding and use of tactile signals from the fingertips in object manipulation tasks," *Nat. Rev. Neurosci.*, vol. 10, no. 5, pp. 345–359, 2009.

[32] J. R. Flanagan, P. Vetter, R. S. Johansson, and D. M. Wolpert, "Prediction precedes control in motor learning," *Curr. Biol.*, vol. 13, no. 2, pp. 146–50, 2003.

[33] J. R. Flanagan, M. C. Bowman, and R. S. Johansson, "Control strategies in object manipulation tasks," *Curr. Opin. Neurobiol.*, vol. 16, no. 6, pp. 650–659, 2006.

[34] N. Hogan, E. Bizzi, F. A. Mussa-Ivaldi, and T. Flash, "Controlling multijoint motor behavior," *Exercise Sport Sci. Rev.*, vol. 15, pp. 153–190, 1987.

[35] M. Kawato, "Internal models for motor control and trajectory planning," *Curr. Opin. Neurobiol.*, vol. 9, no. 6, pp. 718–727, 1999.

[36] S. Dosen, M. Markovic, K. Somer, B. Graimann, and D. Farina, "EMG Biofeedback for online predictive control of grasping force in a myoelectric prosthesis," *J. Neuroeng. Rehabil.*, vol. 12, no. 1, p. 55, 2015.

[37] C. Cipriani, J. L. Segil, J. A. Birdwell, and R. F. ff Weir, "Dexterous control of a prosthetic hand using fine-wire intramuscular electrodes in targeted extrinsic muscles," *IEEE Trans. Neural Syst. Rehabil. Eng.*, vol. 22, no. 4, pp. 828–836, Jul. 2014.